Numerical modelling of wave attenuation through soil

Modélisation numérique de la propagation dans le sol des vibrations

R. Colombero[*1], S. Kontoe[2], S. Foti[1] and D. M. Potts[2]

[1] *Politecnico di Torino, Torino, Italy*
[2] *Imperial College, London, United Kingdom*
[*] *Corresponding Author*

ABSTRACT Numerical analyses of induced ground vibrations play an important role in assessing building safety and comfort. One of the major difficulties is related to the calibration of an adequate source model to be used in the numerical simulation. In this paper the attenuation of waves caused by drop load tests is considered to provide a general framework for the evaluation of vibration attenuation both with empirical laws and numerical simulations. A new equation to reproduce the source signal is suggested and used as input for a dynamic coupled consolidation Finite Element Analysis. The model is validated through comparison with field data obtained at a site in the vicinity of the Tower of Pisa, Italy, from geophones at various distances from the impact source. The calibrated numerical model is then used to study in detail the attenuation of waves from the source and assess the validity of empirical attenuation laws.

RÉSUMÉ La modélisation numérique de vibrations induites dans le sol joue un rôle important dans l'évaluation de la sécurité et le confort des constructions. L'une des principales difficultés à cet égard est le calibrage d'un adéquat modèle pour représenter la source dans la simulation numérique. Dans cet article, l'atténuation des ondes causées par les drop load tests est considérée comme la base pour une général évaluation de l’atténuation des vibrations pas comparaison avec lois empiriques et simulations numériques. Une neuve équation pour reproduire le signal de la source est présentée et utilisée dans une analyse par éléments finis en tenant compte de la consolidation dynamique. Le modèle est validé par comparaison avec les données de mesures obtenues sur un site à proximité de la Tour de Pisa, en Italie, du géophones à différentes distances de la source des vibrations. Le modèle numérique calibré est ensuite utilisé pour étudier en détail l'atténuation des ondes propageant dans le sol et pour évaluer la validité des lois d'atténuation empiriques.

1 INTRODUCTION

Surface wave tests, including drop load tests, are often used for site characterisation (Foti et al. 2014). These tests are non-intrusive and can be used to obtain shear wave velocity and material damping profiles at a site.

Several analytical expressions have been developed in the past to reproduce the source pulse generated by drop load tests (Pekeris 1955; Mooney 1974; Abe et al. 1990). However, only a few of these provide a good match to real data. As the influence of the drop load apparatus set-up is found dominant on the resultant wave field, a new expression for the disturbing source signal is proposed, based on experimentally recorded signals, generated by a well characterised source.

Several factors contribute to the attenuation of the vibration amplitude with the distance in the ground. The most important contributions are given by geometrical wave spreading, material damping and scattering due to heterogeneities in the soil: the first component following a power law with the distance from the source, the latter two an exponential law (Auersch 2010).

Numerical simulations of the case study of Pisa, Italy, were carried out to validate wave velocity-distance attenuation relationships. The layered soil profile was modelled in detail in the finite element model and the input drop load action was based on a novel expression for the disturbing source pulse. The numerical model was considered to be reliable in reproducing the attenuation of the wave generated by drop load tests, as a very good agreement between the experimental and the computed peak particle velocity (PPV) decay trends with distance was achieved.

2 AMPLITUDE-DISTANCE ATTENUATION LAWS

2.1 Theoretical framework

Any disturbing source, as simple as an impulse, acting on a medium generates a complex wave field. The amplitude of such waves decays with distance as the waves propagate away from the source. Two are the main mechanisms that influence the attenuation of impact-induced vibrations (Semblat & Pecker 2009; Auersch 2010):

- Geometrical attenuation: based on the elastic wave energy conservation, the amplitude A of waves generated at a point attenuate with distance r following a power law $A \propto r^{-n}$, where A represents the wave velocity amplitude and r is the distance from the source position. The exponent n takes values of 0.5 or 2.0 respectively for surface and body waves produced by a surface point load (Auersch 2010).
- Material attenuation and scattering in non-homogeneous media: the hysteretic behaviour of the soil and the wave refraction at interfaces between layers lead to a second attenuation component, exponentially dependent on the distance, $\mathrm{A} \propto \exp(\text{-k} \cdot \mathrm{r})$, where the coefficient k accounts for material damping, soil natural frequency and surface waves characteristics (Auersch 2010).

2.2 Amplitude-distance attenuation laws for waves induced by impact loads

It has been argued that the exponential term has only a minor influence on the energy reduction of ground vibrations induced by impact sources as the distance increases (Auersch & Said 2010). Hence it can be neglected and the attenuation of the vibrations can be approximated by a power law of similar form to the theoretical one: $A \propto r^{-q}$. Various experimental velocity recordings have been analysed to assess the attenuation of impact-induced vibrations and the exponent q was found to change according to the type of source and type of soil profile (Auersch & Said 2010). The experimental exponent q has been found varying between values of 1.0 and 1.6 for drop load tests carried out on sandy and clayey soils respectively (Auersch 2010).

Further experimental studies (Mooney 1976) correlate the vibration amplitude A of the induced wavefield with the distance r from the disturbing source through a power law and with the characteristics of the source as defined below:

$$A = C \cdot H_S \cdot r^{-n} \cdot T_S{}^{-m-p} \tag{1}$$

Where H_S and T_S are the source pulse and period respectively; C is a constant; $m+p$=1.4 and n=0.5 are the surface wave velocity exponents.

Equation (1) can be expanded taking into account also the effect given by the exponential term to obtain a complete attenuation law that can be applied to drop load tests:

$$A = C \cdot H_S \cdot R^{-n} \cdot T_S{}^{-m-p} \cdot exp(-kR) \tag{2}$$

Where $k = 2\pi\xi$ (with ξ material damping); n is the effective surface wave velocity attenuation exponent; and $R = r/\lambda_R$, with λ_R the surface waves wavelength.

3 DROP LOAD TESTS AND ANALYTICAL REPRESENTATION OF DISTURBING SOURCES

Drop load tests consist of a falling heavy weight hitting a plate or directly the ground, generating a wave field. Particle velocity signals are captured at different distances from the source by geophones (Foti 2000; Figure 1).

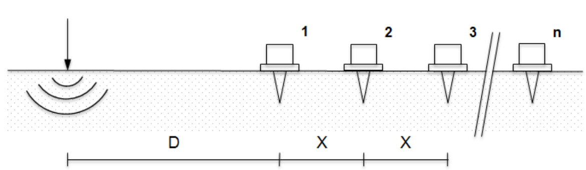

Figure 1. Experimental setup for multistation SASW tests

Early attempts to evaluate the soil response due to a surface point force were based on the disturbing action represented by a vertical impulse (Lamb 1904; Mooney 1974), a step unit function (Pekeris 1955) or sinusoidal functions (Mooney 1974; Abe et al. 1990).

In the latest studies the amplitude of the source signal was found proportional to the momentum of the weight before the impact (given by the product of mass by velocity just before the impact).

From the analysis of near-field observations of particle velocity time histories recorded by geophones, a new more accurate expression is derived. A Gabor wavelet (Semblat & Pecker 2009) formed the basis of the new function, then modified to account for the momentum of the dropped weight C_b in order to approximate the pulse produced by a mass falling on the ground (Figure 2, equation (3)).

$$v(t) = \begin{cases} C_b \cdot \beta \cdot t^{\gamma} \cdot exp\left[-\left(\frac{2\pi}{T_S\alpha}t\right)^2\right] cos\left(\frac{2\pi}{T_S}t\right), & 0 \le t \le 1.2T_S \\ 0, & otherwise \end{cases} \quad (3)$$

where t is a generic time instant; T_S the period of the function; and α, β, and γ are constants.

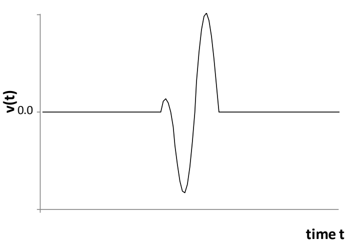

Figure 2. Modified Gabor wavelet

4 SITE DESCRIPTION AND FIELD DATA

The subsoil of Piazza dei Miracoli, Pisa (Italy) has been extensively characterised in the last decades as the basis for the stabilisation design of the Tower.

The soil stratigraphy beneath Piazza dei Miracoli presents a sequence of sand and clay formations and is represented in Figure 3. Seismic Analysis of Surface Waves tests (SASW), among which drop load tests, were performed in Piazza dei Miracoli next to the Tower (Foti 2003).

The drop load test configuration consisted of a 130 kg weight dropped from a height of approximately 3 m, hitting the ground directly in order to avoid mass rebound and to reach lower frequencies. The vibrations at the surface were recorded by 24 in-line geophones at 2.5m spacing.

Figure 4 shows the velocity time histories recorded at 5, 35 and 60m from the source location. The increase in the significant duration of the motion with distance is due to increasing shear wave velocity with depth, i.e. the dispersive behaviour of the soil, typical of heterogeneous media.

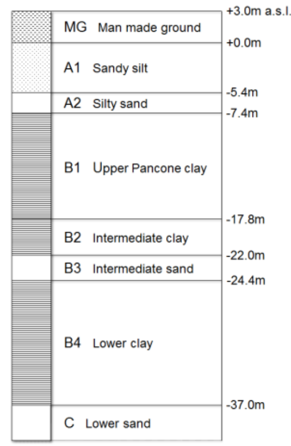

Figure 3. Indicative stratigraphy retrieved in Piazza dei Miracoli, Pisa

5 NUMERICAL MODEL DESCRIPTION

Fully coupled finite element simulations of the drop-load tests carried out in Pisa were performed in the time domain with the code ICFEP (Potts & Zdravkovic 2001). The precise evaluation of the model input parameters is of primary importance for the accurate representation of the impact-induced wavefield.

The domain discretisation for the simulation of the drop load tests consisted of: two-dimensional axisymmetric configuration; mesh dimensions 160m x 53m; total number of 9472 eight-noded quadrilateral solid elements to define the mesh; horizontal displacements restricted along the left lateral boundary to account for symmetry of the problem; tangential and normal to boundary dashpots applied at the bottom and right lateral boundaries to absorb wave reflections; zero pore pressure at water table depth (assumed 1.3m bgl); and disturbing action applied at the top left node of the model.

As the impact source used in the tests performed in Pisa was not monitored, the modified formulation of the Gabor wavelet (Semblat & Pecker 2009, equation (3)) was considered as the model synthetic input source signal, employing the following parameters:

$\alpha = 7$; $\beta = 1.55 \cdot 10^{-2}$; $\gamma = 1.2$; $T_S = 0.04s$; and $C_b = 997.4\, kg \cdot m/s$. These parameters were obtained with a calibration on the signal at the first geophone.

The properties assigned to the materials are shown in Table 1. The material damping of the soil profile was approximated with the Rayleigh damping formulation, based on a target damping ratio varying with depth (Foti 2003). Incomplete saturation of near-surface layers was also approximated in the analyses (Table 2) by appropriately reducing the corresponding pore fluid compressibility.

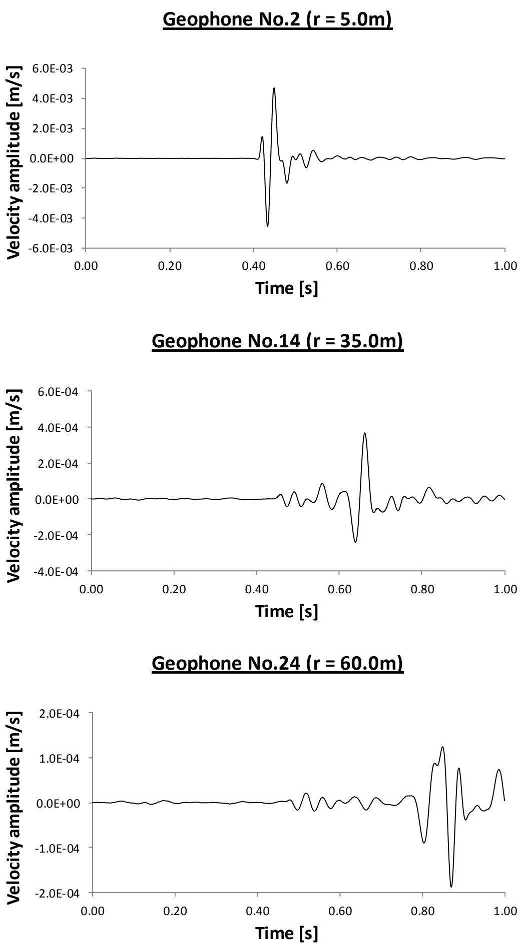

Figure 4. Velocity time histories recorded at r = 5, 35 and 60 m from the source

Table 1. Soil properties used in the finite element analysis – Vs: shear wave velocity; γ: bulk unit weight; E: soil stiffness; ν: Poisson's Ration; ξ*: target damping ratio; K: permeability

Layer	V_s [m/s]	γ [kN/m3]	E [MPa]	ν [/]	ξ* [%]	K [m/s]
MG	155	19.00	124	0.33	7.0	1E-07
A1	180	18.50	163	0.33	5.4	1E-07
A2	170	18.00	141	0.33	2.5	5E-07
BI	150	16.75	102	0.33	3.1	9E-09
BII	235	19.50	2920	0.33	2.0	8E-09
BIII	245	18.75	3051	0.33	2.0	5E-07
BIV	215	18.00	226	0.33	2.0	8E-09
C	380	20.00	783	0.33	2.0	5E-7

Table 2. Partial saturation characteristics - K_f: bulk modulus of fluid and S_r: correspondent saturation

Layer	K_f [kPa]	S_r [%]
Layer MG (above water table)	9954.8	99.00%
Layer MG (below water table)	19819.8	99.50%
Layer A1 (Vp <1400 m/s, 6m bgl)	592710.5	99.981%
Layer A1 (Vp >1400 m/s)	2.2E6	100.00%
Layers A2 ÷ C	2.2E6	100.00%

6 RESULTS

The results from the finite element simulation have been compared with the field measurements. To get a representative response for near-field, far-field and intermediate conditions, geophones at 5m, 35m and 60m distance from the disturbing source are reported.

6.1 Comparison with the field data

The experimental recordings at the geophones are compared to the numerical results in Figure 5.

High resemblance is achieved between the signals, in particular in the near- and middle-field, while in the far-field a faster wavefield propagation in the soil is predicted. The waves of smaller amplitude (registered after the major tremor) due to wave reflections and refractions in the soil deposit are not well captured by the numerical model. These inaccuracies in the response are mainly due to the simplifications used in the numerical model, e.g. uncertainties in the degree of soil saturation and the use of a synthetic source signal based on a single central frequency (25 Hz).

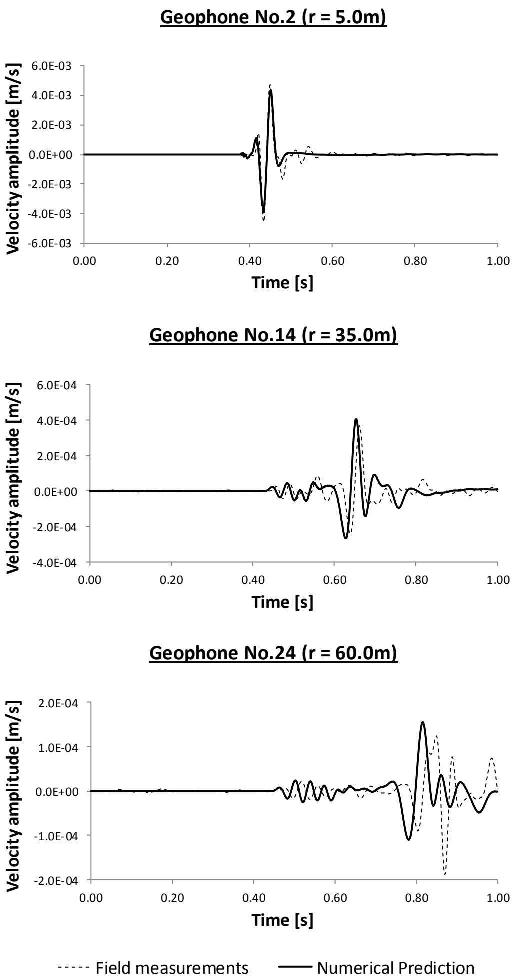

Figure 5. Comparison of the experimental and numerical time histories (at r = 5, 35 and 60 m from the source)

6.2 Comparison of the PPV trend with literature equations

The most effective approach to analyse the attenuation of ground vibrations is the analysis of the peak particle velocities (PPVs) recorded by each geophone. The magnitude of the peak particle velocities recorded in Pisa decreases from 9 mm/s at a distance of 2.5 m from the source to 0.2 mm/s at a distance of 60 m (Figure 6, white circles).

The previously mentioned analytical and empirical attenuation equations are presented for comparison. In Figure 6 both experimental data and numerical predictions are approximated by the power law $A \propto r^{-q}$, which gives a straight line on a double logarithmic plane with slope $q = 1.282$ and $q = 1.272$ respectively. An accurate modelling has therefore been achieved and this power attenuation law is found to be able to reproduce the wave amplitude decay with sufficient accuracy for preliminary design purposes. A second comparison is made against the complete attenuation law given by equation (2) for both experimental and numerical data (Figure 7 and Figure 8 respectively). The input coefficients are $T_S = 0.04s$; $H_S = 0.145\,mm/s$; $k = 0.302$; $C = 3800$; $m + p = 1.4$; and $n = 0.75$.

The very good agreement between the complete law and the measured attenuation trend demonstrates the importance of the exponential component, related to the soil material, to the overall attenuation.

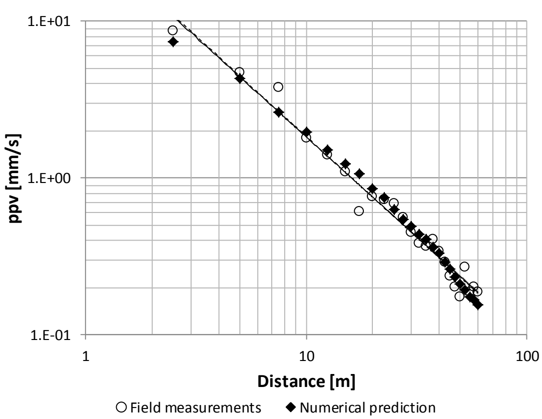

Figure 6. Comparison of the experimental and numerical PPV attenuation curves

7 CONCLUSIONS

This study investigated the attenuation of ground vibrations generated by drop load tests and compared analytical and empirical expressions with the attenuation predicted by numerical analysis using as a reference the field data from the well-documented case study of Pisa.

The soil response due to a weight falling on the ground has been investigated in previous studies. The

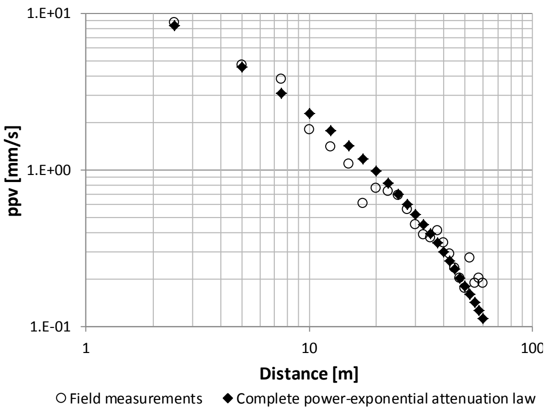

Figure 7. Comparison of the field measurements attenuation curve with the amplitude-distance curve given by equation (2)

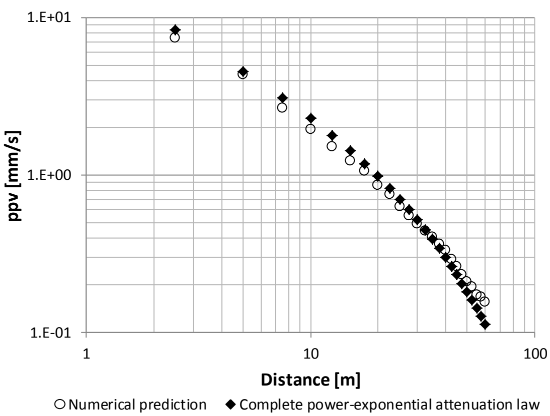

Figure 8. Comparison of the numerical PPV attenuation curve with the amplitude-distance curve given by equation (2)

simplified source signal and homogeneous soil representation previously proposed were revised to obtain a better representation of the disturbing action produced by drop load tests. A new expression (equation (3)) is presented which for the examined case study was shown to successfully represent the impact source, but further analysis is needed to confirm its applicability.

Two main factors contribute to the attenuation of impact-induced waves in the ground: geometrical spreading and material damping, following a power and exponential attenuation law respectively. Numerous equations have been suggested in previous studies to reproduce the decay of the waves with distance. A simplified power law and a complete power-exponential law were examined in this study. Both expressions exhibited good agreement with the field data of drop load tests carried out in Pisa, but the superiority of the complete law was evident.

As an independent assessment of the existing analytical attenuation expressions, a numerical simulation of the drop load tests was performed with the finite element program *ICFEP* (Potts and Zdravkovic 2001). The agreement of the numerical results with the experimental recordings shows how an excellent prediction of the induced ground vibrations can be achieved on the basis of a good site characterisation and a monitoring device close to the source.

REFERENCES

Abe, S. Kobayashi, Y. & Ikawa, T. 1990. Seismic characteristics of the weight-dropping source. *Journal of Physics of the Earth* **38** (3), 189-212.

Auersch, L. 2010. Technically Induced Surface Wave Fields, Part I: Measured Attenuation and Theoretical Amplitude-Distance Laws. *Bulletin of the Seismological Society of America* **100** (4), 1528-1539.

Auersch, L. & Said, S. 2010. Attenuation of ground vibrations due to different technical sources. *Earthquake Engineering and Engineering Vibration* **9** (3), 337-344.

Foti, S. 2003. Small-strain stiffness and damping ratio of Pisa clay from surface wave tests. *Geotechnique* **53** (5), 455-461.

Foti, S. 2000. Multistation methods for geotechnical characterization using surface waves. *PhD Degree in Geotechnical Engineering, Department of Structural and Geotechnical Engineering*. Technical University of Turin (Politecnico), Italy.

Foti S. Lai C.G. Rix G.J. & Strobbia C. 2014. *Surface Wave Methods for Near-Surface Site Characterization.* CRC Press, Boca Raton, Florida (USA).

Lamb, H. 1904. On the propagation of tremors over the surface of an elastic solid. *Philosophical Transactions of the Royal Society of London. Series A, Containing papers of a mathematical or physical character* **203**, 1-42.

Mooney, H. M. 1976. The seismic wave system from a surface impact. *Geophysics* **41** (2), 243-265.

Mooney, H. M. 1974. Some numerical solutions for Lamb's problem. *Bulletin of the Seismological Society of America* **64** (2), 473-491.

Pekeris, C. 1955. The seismic surface pulse. *Proceedings of the National Academy of Sciences of the United States of America* **41** (7), 469.

Potts, D.M. & Zdravković, L. 2001. *Finite element analysis in geotechnical engineering: theory*. Thomas Telford, London.

Semblat, J.J. & Pecker, A. 2009. *Waves and vibrations in soils*. Iuss Press, Pavia.